

Effect of Surface Film Structure on the Quartz Crystal Microbalance Response in Liquids

Leonid Daikhin and Michael Urbakh*

School of Chemistry, Raymond and Beverly Sackler Faculty of Exact Sciences,
Tel-Aviv University, 69978 Ramat-Aviv, Tel-Aviv, Israel

Received September 13, 1995. In Final Form: October 1, 1996[®]

The effect of surface roughness and the morphology of nonuniform surface films on a quartz crystal microbalance (QCM) response in liquids has been investigated. Our description of the velocity field in the interfacial region is based on Brinkman's equation, commonly employed in the treatment of a flow through porous media. In this approach one treats the flow of a liquid through a nonuniform surface layer as the flow of a liquid through a porous medium. The morphology of the interfacial layer is characterized by the permeability that depends on the "porosity" of the layer. The model proposed here gives a unified approximate description of the QCM response for various scales of roughness. It includes both the effect of viscous dissipation in the interfacial layer and the effect of the liquid mass rigidly coupled to the surface. A relation between the QCM response and the interface geometry has been found. The model discussed here can be used for the treatment of QCM response of rough electrode surfaces, of porous deposited films, and of surface polymer films.

Introduction

Oscillating quartz crystals have been employed as piezoelectric bulk acoustic wave (BAW) sensors of the thickness shear mode (TSM) variety to investigate interfacial processes at surfaces and in thin films.¹ The TSM resonator is commonly called a quartz crystal microbalance (QCM). In the last few years there has been increased attention to the application of QCM for studies of solid-liquid interfaces.^{2,3} It was successfully demonstrated that QCM can serve as a sensitive tool to probe interfacial friction,⁴ thin film viscoelasticity,^{5,6} polymer film properties,³ and a bulk liquid viscosity and density.^{7,8} The combination of the QCM technique with electrochemical methods has made possible *in situ* measurements of minute mass changes that take place during adsorption, underpotential deposition, dissolution of surface films, and other electrochemical processes.^{3,9,10} In most of these investigations, frequency changes were interpreted in terms of rigid mass changes, based on the Sauerbrey equation.¹¹ In liquids, however, the QCM response depends on various factors such as an electrode microstructure, a morphology of surface films, interfacial liquid properties, and on the solid-liquid coupling at the interface. In many cases frequency changes are not consistent with the predictions given by Sauerbrey equations,^{2,12,13} and a detailed theoretical analysis is needed to extract information from the experimental results.

Progress has been made in characterizing the response of a smooth resonator operating in contact with a Newtonian liquid.^{7,8,14} The oscillating surface generates plane-parallel laminar flow in the liquid that causes a decrease in the resonant frequency and the resonator damping proportional to $(\rho\eta)^{1/2}$ where ρ and η are the liquid density and viscosity. The influence of surface microstructure on the QCM response in contact with liquids has only begun to be investigated.^{15–23} When the surface of the resonator is rough, the liquid motion generated by the oscillating surface becomes much more complicated than for the smooth surface. A variety of additional mechanisms of coupling between acoustic waves and a liquid motion can arise, such as the generation of a nonlaminar motion, the conversion of the in-plane surface motion into the surface-normal liquid motion, and the trapping of liquid by cavities and pores. It has been experimentally demonstrated^{16–18,20,21} that roughness-induced shift of the resonant frequency includes both the inertial contribution due to the liquid mass rigidly coupled to the surface and the contribution due to the additional viscous energy dissipation caused by the nonlaminar motion in the liquid. Measurements of the complex shear mechanical impedance²⁰ have been used to analyze different contributions to the roughness-induced response of the quartz resonator and to correlate the experimental results with the device roughness. Nevertheless, this subject is highly undeveloped, and the interpretation of experimental results is ambiguous, which prevents the

* To whom correspondence should be addressed. E-mail: urbakh@ccsg.tau.ac.il.

® Abstract published in *Advance ACS Abstracts*, December 1, 1996.

(1) Lu, C.; Czanderna, A. W., Eds. *Applications of Piezoelectric Quartz Crystal Microbalances*; Elsevier: Amsterdam, 1984.
(2) Thompson, M.; Kipling, L. A.; Duncan-Hewitt, W. C.; Rajakovic, L. V.; Cavic-Vlasak, B. A. *Analyst* **1991**, *116*, 881.
(3) Buttry, D. A.; Ward, M. D. *Chem. Rev.* **1992**, *92*, 1355.
(4) Watts, E. T.; Krim, J.; Widom, A. *Phys. Rev. B* **1990**, *41*, 3466.
(5) Johannsmann, D.; Mathauer, K.; Wegner, G.; Knoll, W. *Phys. Rev. B* **1992**, *46*, 7808.
(6) Reed, C. E.; Kanazawa, K. K.; Kaufman, J. H. *J. Appl. Phys.* **1990**, *68*, 1993.
(7) Bruckenstein, S.; Shay, M. *Electrochim. Acta* **1985**, *30*, 1295.
(8) Kanazawa, K. K.; Gordon, J. G., II. *Anal. Chim. Acta* **1985**, *175*, 99.
(9) Buttry, D. A. In *Electroanalytical Chemistry*; Bard, A. J., Ed.; Marcel Dekker: New York, 1991; Vol. 17, p 1.
(10) Schumacher, R. *Angew. Chem., Int. Ed. Engl.* **1990**, *29*, 329.
(11) Sauerbrey, G. *Z. Phys.* **1959**, *155*, 206.
(12) Kipling, A. L.; Thompson, M. *Anal. Chem.* **1990**, *62*, 1514.

(13) Rajakovic, L. V.; Cavic-Vlasak, B. A.; Ghaemmaghami, V.; Kallury, M. R. K.; Kipling, A. L.; Thompson, M. *Anal. Chem.* **1991**, *63*, 615.

(14) Beck, R.; Pittermann, U.; Weil, K. G. *Ber. Bunsen-Ges. Phys. Chem.* **1988**, *92*, 1363.

(15) Yang, M.; Thompson, M.; Duncan-Hewitt, W. C. *Langmuir* **1993**, *9*, 802.

(16) Beck, R.; Pittermann, U.; Weil, K. G. *J. Electrochem. Soc.* **1992**, *139*, 453.

(17) Yang, M.; Thompson, M. *Langmuir* **1993**, *9*, 1990.

(18) Schumacher, R.; Borges, G.; Kanazawa, K. K. *Surf. Sci.* **1985**, *163*, L621.

(19) Schumacher, R.; Gordon, J. G.; Melroy, O. *J. Electroanal. Chem.* **1987**, *216*, 127.

(20) Martin, S. J.; Frye, G. C.; Ricco, A. J.; Sentaria, S. D. *Anal. Chem.* **1993**, *65*, 2910.

(21) Bruckenstein, S.; Fensore, A.; Li, Z.; Hillman, A. R. *J. Electroanal. Chem.* **1994**, *370*, 189.

(22) Urbakh, M.; Daikhin, L. *Phys. Rev. B* **1994**, *49*, 4866.

(23) Urbakh, M.; Daikhin, L. *Langmuir* **1994**, *10*, 2839.

QCM technique from being widely employed as an analytical tool for studies of solid-liquid interfaces.

It is impossible at the present time to provide a unified description of the QCM response for nonuniform solid-liquid interfaces with an arbitrary geometrical structure. The limiting case of slightly rough surfaces has been considered in our recent works.^{22,23} The calculations demonstrated the generation of the liquid motion normal to the surface oscillations and the nonuniform distribution of the liquid pressure in the interfacial layer. In this case both inertial and viscous components contribute to the roughness-induced QCM response. The quantitative relation between the observable quantities (the resonance frequency shift and width) and the surface morphology have been found.^{22,23}

In the present paper, we derive the coarse-grained description of the liquid motion generated by the oscillations of rough solid surfaces. Our description of the velocity field in the interfacial region is based on Brinkman's equation, commonly employed in the treatment of a flow through porous media.²⁴⁻²⁸ In this approach, which has been also successfully used to discuss the hydrodynamics of polymeric systems,²⁹⁻³¹ one treats the flow of a liquid through a nonuniform surface layer as the flow of a liquid through a porous medium. The morphology of the interfacial layer is characterized by a local permeability that depends on the "porosity" of the layer. The model proposed here gives a unified approximate description of the QCM response for various scales of roughness. It includes both the effect of viscous dissipation in the interfacial layer and the effect of the liquid mass rigidly coupled to the surface. The model discussed here can be also used for the treatment of QCM response of porous deposited films and of surface polymer films. It should be noted that similar coarse-grained models have been employed extensively for the consideration of optical and elastic properties of rough surfaces and nonuniform films.³²

The Model

We now consider a model for the coupling of shear waves in a quartz crystal with damped waves in the nonuniform interfacial layer and in the bulk liquid (see Figure 1). We plot a z -axis pointing toward the liquid and the plane $z = 0$ being coincident with the unconstrained face of the quartz resonator. The second constrained face of the resonator coincides with the plane $z = d$. We consider the liquid side as a two-layer system: the nonuniform interfacial layer located in the region $d < z < L$ and the bulk liquid occupying the semispace $z > L$.

The solution of the wave equation describing the shear time-harmonic displacements in the quartz crystal, $\mathbf{u}(\mathbf{r}, t) = \mathbf{u}(\mathbf{r}, \omega) \exp(i\omega t)$, has the following form

$$u_x(\mathbf{r}, \omega) = V_0 \cos(kz)/(i\omega \cos(kd)), \quad k = \omega(\rho_q/\mu_q)^{1/2}$$

$$u_y(\mathbf{r}, \omega) = 0 \quad \text{and} \quad u_z(\mathbf{r}, \omega) = 0 \quad (1)$$

Here, μ_q and ρ_q are the shear modulus and the density of the quartz crystal, ω is the angular frequency of oscillations, V_0 is the amplitude of the velocity oscillation of the

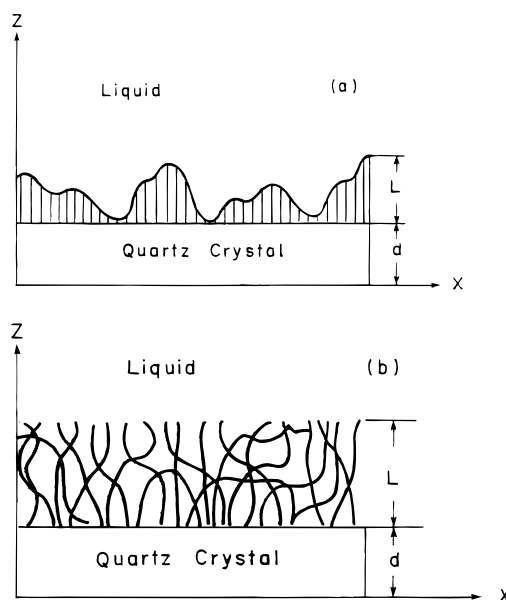


Figure 1. Schematic sketch of interfacial geometries: (a) rough interfacial layer, (b) polymer surface film.

constrained quartz surface, and d is the thickness of the resonator. The coordinate system is defined such that the shear stress lies along the x direction in the x - y plane.

For hydrodynamic purposes we treat the interfacial layer as a two-phase (solid-liquid) porous medium²⁴⁻³¹ with a permeability of ξ_H^2 . Physical meaning of the permeability length scale, ξ_H , depends on the nature of the interfacial layer. For instance, in the case of rough surface layers ξ_H is related to their porosity, and for an entangled polymer layer ξ_H is of the same magnitude as the equilibrium correlation length.³³ The local permeability ξ_H^2 can change with the distance from the quartz surface.³⁰ Here, for simplicity, we do not consider this effect. In our model ξ_H^2 presents an average permeability of the layer.

We assume that the solid phase (surface roughnesses, a porous deposit, a polymer film) is rigidly coupled to the crystal surface and oscillates with the velocity $V_0 \exp(i\omega t)$. The liquid flow through the interfacial layer, $v_x(z, t) = v_x(z, \omega) \exp(i\omega t)$, is described by Brinkman's equation²⁴⁻²⁸

$$i\omega \rho v_x(z, \omega) = \eta \frac{d^2}{dz^2} v_x(z, \omega) + \eta \xi_H^{-2} (V_0 - v_x(z, \omega)) \quad (2)$$

where ρ and η are the liquid density and viscosity, respectively. In this equation the effect of the solid phase on the liquid flow is given by the resistive force that has a Darcy-like form, $\eta \xi_H^{-2} (V_0 - v_x(z, \omega))$.

Darcy's law and Brinkman's equation (2) have been derived under the following assumptions:²⁵⁻²⁸ (a) low Reynolds number, $Re = (\omega a \rho)/\eta \leq 1$, where a is the amplitude of the quartz oscillation; (b) nonslip boundary conditions at solid-liquid interfaces; and (c) the characteristic size of inhomogeneities, r , less than the thickness of the interfacial layer, L . It should be noted that the derivation of Brinkman's equation does not impose restrictions on the relation between decay length for the shear wave launched into the liquid phase, $\delta = (2\eta/\omega\rho)^{1/2}$, and other characteristic lengths in our problem, ξ_H and r .

Brinkman's equation presents a variant of the effective medium approximation that does not describe explicitly the generation of nonlaminar liquid motion and conversion of the in-plane surface motion into the normal-to-interface

(33) For entangled polymer the correlation length is the average distance between entanglement points.

(24) Brinkman, H. C. *Appl. Sci. Res. A* **1947**, 1, 27.
 (25) Sahimi, M. *Rev. Modern Phys.* **1993**, 65, 1393 (page 1440).
 (26) Hilfer, R. In *Advances in Chemical Physics*; Prigogine, I.; Rice Stuart, A., Eds.; John Wiley & Sons, Inc.: New York, 1996; Vol. 92, p 299.
 (27) Tam, C. K. W. *J. Fluid. Mech.* **1969**, 38, 537.
 (28) Lundgren, T. S. *J. Fluid. Mech.* **1972**, 51, 273.
 (29) de Gennes, P. G. *Macromolecules* **1981**, 14, 1637.
 (30) Fredrickson, Glenn H.; Pincus, P. *Langmuir* **1991**, 7, 786.
 (31) Jones, L. G.; Marques, C. M.; Joanny, J.-F. *Macromolecules* **1995**, 28, 136.
 (32) Hunderi, O. *Surf. Sci.* **1980**, 96, 1.

liquid motion. These effects result in additional channels of energy dissipation that are effectively included into the model by the introduction of the Darcy-like resistive force. It should be noted that QCM response discussed here is sensitive to the energy dissipation rather than to the details of the velocity field in the liquid. While the limitation of Brinkman's equation are apparent, there is no alternative equation in the literature that has been accepted unconditionally.

A number of relations for the permeability ξ_H^2 have been proposed on the basis of both model calculations and empirical considerations.²⁵ For instance, the empirical Kozeny–Carman equation

$$\xi_H^2 \propto r^2 \phi^3 / (1 - \phi)^2$$

expresses the permeability in terms of the characteristic size of inhomogeneities, r , and of the porosity, ϕ , which is the volume fraction of the liquid phase in the interfacial layer.

In the case of high porosity, $\phi \approx 1$, the resistive force is small and eq 2 reduces to the Navier–Stokes equation describing the motion of a liquid in contact with a smooth quartz surface. The resistive force increases with the decrease of the porosity and strongly influences the motion of the liquid in the interface region. At very low porosity, $\phi \ll 1$, all liquid located in the layer is trapped by roughness and moves with the velocity that is equal to the velocity of the crystal surface.

In the case of thick polymer films the hydrodynamic equation (2) should be augmented with a description of the polymer network elasticity. However, in the most of QCM experiments³ the thickness of polymer films is less than the wavelength of shear oscillations, and the polymer can be considered as rigidly coupled to the surface. For grafted polymer brushes the length ξ_H has the order of the equilibrium concentration correlation length,^{29–31} which is proportional to $c^{-3/4}$, where c is the average monomer concentration.

In the frame of the approximation discussed here the system is treated as macroscopically homogeneous along the surface plane x – y . The only inhomogeneity takes place in the z -direction normal to the surface of the quartz crystal. In writing eq 2 we have taken into account that the pressure is constant for systems that are homogeneous along the plane of oscillation.

The plane-parallel laminar flow generated in the bulk liquid is described by the velocity field $v_x(\mathbf{r}, \omega)$ that is the solution of the linearized Navier–Stokes equation³⁴

$$v_x(\mathbf{r}, \omega) = v_x(L) \exp(-q_0(z - L)) \quad (3)$$

where $q_0 = (i\omega\rho/\eta)^{1/2}$.

Boundary conditions for the velocity field in the liquid include (a) the nonslip boundary condition at the interface $z = d$: $v_x(d, \omega) = V_0$; (b) the continuity of the liquid velocity at the interface $z = L$; and (c) the equality of the absolute values and the opposite directions of the shear stresses on two sides of the interface $z = L$:

$$\frac{dv_x(z, \omega)}{dz} \Big|_{z=L-0} = \frac{dv_x(z, \omega)}{dz} \Big|_{z=L+0}$$

After the determination of the velocity profile in the interfacial layer and in the bulk liquid the resonance frequency shift and width can be found from the energy balance in the system under consideration.^{22,23} The rate of the change of the kinetic ($E_{\text{kin}}^{(q)}$) and the elastic ($U^{(q)}$)

energy of the quartz crystal and the kinetic energy of the liquid both in the interfacial layer ($E_{\text{kin}}^{(s)}$) and in the bulk ($E_{\text{kin}}^{(b)}$) should be equal to the rate of the energy dissipation in the layer ($Q^{(s)}$) and in the bulk ($Q^{(b)}$)

$$\frac{d}{dt}(E_{\text{kin}}^{(q)} + U^{(q)} + E_{\text{kin}}^{(s)} + E_{\text{kin}}^{(b)}) = Q^{(s)} + Q^{(b)} \quad (4)$$

The expressions for the energetic terms in eq 4 have the form

$$E_{\text{kin}}^{(q)} = \frac{\rho_q}{2} \int dz \left(\frac{\partial}{\partial t} u_x(z, t) \right)^2 \quad (5)$$

$$U^{(q)} = \frac{\mu_q}{2} \int dz \left(\frac{\partial}{\partial z} u_x(z, t) \right)^2 \quad (6)$$

$$E_{\text{kin}}^{(s)} = \frac{\rho}{2} \int_d^L dz (v_x(z, t))^2; \quad E_{\text{kin}}^{(b)} = \frac{\rho}{2} \int_L^\infty dz (v_x(z, t))^2 \quad (7)$$

$$Q^{(s)} = -\eta \int_d^L dz \left(\frac{\partial}{\partial z} v_x(z, t) \right)^2 + \xi_H^{-2} (V_0 \exp(i\omega t) - v_x(z, t))^2 \quad (8)$$

$$Q^{(b)} = -\eta \int_L^\infty dz \left(\frac{\partial}{\partial z} v_x(z, t) \right)^2 \quad (9)$$

The expression (8) for the energy dissipation rate in the surface layer results from Brinkman's equation (2) (see Appendix). The second term in the right hand side (rhs) of eq 8 presents the energy dissipation due to the friction between liquid and solid phases in this layer. The contribution corresponding to the kinetic energy of the solid phase of the interfacial layer has not been included in the energy balance (4). This contribution leads to the frequency shift that is proportional to the mass of the solid phase and is given by the Saurbrey equation.

The solution of eq 2 with the boundary conditions a–c can be written as follows:

$$v_x(z, \omega) = V_0 \frac{1}{\xi_H^2 q_1^2} + C_1 \exp(q_1(z - d)) + C_2 \exp(-q_1(z - d)) \quad (10)$$

Here $q_1^2 = q_0^2 + \xi_H^{-2}$, and the coefficients C_1 and C_2 have the form

$$C_1 = \frac{V_0}{2W} \left((q_1 - q_0) \exp(-q_1 L) \left(1 - \frac{1}{\xi_H^2 q_1^2} \right) - \frac{q_0}{\xi_H^2 q_1^2} \right) \quad (11)$$

$$C_2 = \frac{V_0}{2W} \left((q_1 + q_0) \exp(q_1 L) \left(1 - \frac{1}{\xi_H^2 q_1^2} \right) + \frac{q_0}{\xi_H^2 q_1^2} \right) \quad (12)$$

$$W = q_1 \cosh(q_1 L) + q_0 \sinh(q_1 L) \quad (13)$$

Equations 10–13 show that the velocity profile is determined by two parameters: δ/L and ξ_H/L , which are the ratios of the decay length of the velocity field in the bulk liquid, $\delta = (2\eta/\omega\rho)^{1/2}$, and of the permeability length scale, ξ_H , to the thickness of the interfacial layer, L . Figure 2 presents the velocity profiles in the liquid near the quartz crystal surface for different values of the parameters δ/L and ξ_H/L . We see that the effect of the interfacial layer is most pronounced for small values of ξ_H/L . The velocity gradient in the layer decreases with the decrease of ξ_H/L , and for $\xi_H/L \ll 1$ the majority of the layer moves with a

(34) Landau, L. D.; Lifshitz, E. M. *Fluid Mechanics*, 2nd ed.; Pergamon: New York, 1987.

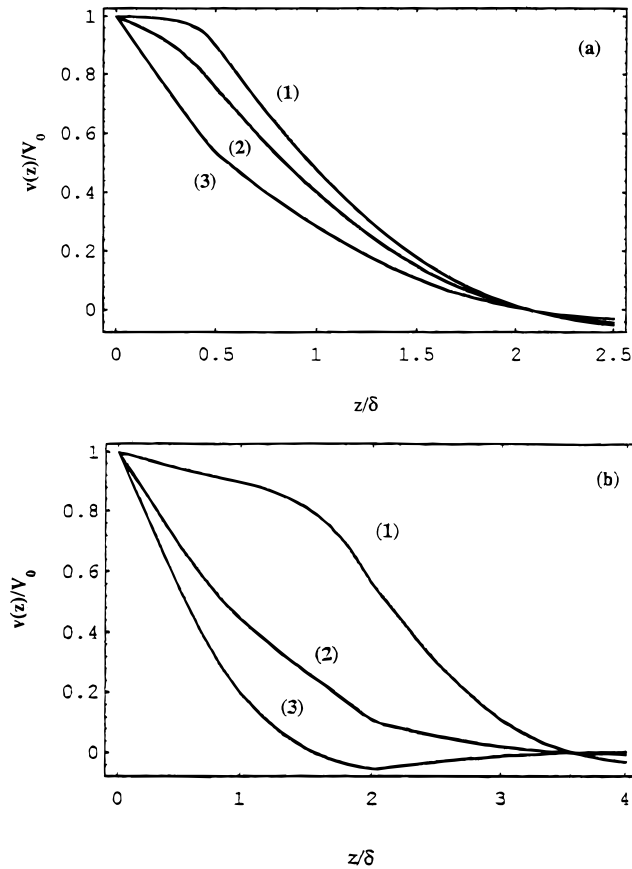


Figure 2. Velocity profiles in the liquid near the quartz crystal surface for two-layer thicknesses: 2a, $L = 0.5\delta$; b, $L = 2\delta$. The calculations were carried out for the following values of the parameters: (1) $\xi_H/L = 0.2$, (2) $\xi_H/L = 0.5$, (3) $\xi_H/L \gg 1$, which corresponds to the smooth solid–liquid interface.

velocity equal to the velocity of the quartz surface, V_0 . This behavior reflects the trapping of the liquid by the surface roughness. For higher values of the parameter $\xi_H/L \geq 1$, the influence of the interfacial layer goes down and the velocity field approaches the velocity field at the smooth solid–liquid interface.

After substitution of eqs 1, 2, and 10–13 into eq 4 we arrived at the following equation for the determination of the resonance frequency:

$$tg(kd) = -\frac{k\rho}{\rho_q q_q} \left\{ 1 + q_0 \frac{L}{\xi_H^2 q_1^2} - \frac{q_1}{W} \frac{1}{\xi_H^2 q_1^2} \times \left[\frac{2q_0^2}{q_1^2} (\cosh(q_1 L) - 1) + \frac{q_0}{q_1} \sinh(q_1 L) \right] \right\} \quad (14)$$

Now the liquid-induced shift, $\Delta\omega$, and the width, Γ , of the resonance frequency may be written in the form

$$\Delta\omega = -\frac{\omega_0^2 \rho}{\pi(\mu_q \rho_q)^{1/2}} \text{Re} \left\{ \frac{1}{q_0} + \frac{L}{\xi_H^2 q_1^2} - \frac{1}{W} \frac{1}{\xi_H^2 q_1^2} \left[\frac{2q_0}{q_1} (\cosh(q_1 L) - 1) + \sinh(q_1 L) \right] \right\} \quad (15)$$

$$\Gamma = -\frac{\omega_0^2 \rho}{\pi(\mu_q \rho_q)^{1/2}} \text{Im} \left\{ \frac{1}{q_0} + \frac{L}{\xi_H^2 q_1^2} - \frac{1}{W} \frac{1}{\xi_H^2 q_1^2} \left[\frac{2q_0}{q_1} (\cosh(q_1 L) - 1) + \sinh(q_1 L) \right] \right\} \quad (16)$$

Here $\Delta\omega = \omega - \omega_0$ and $\omega_0 = (\pi/d)(\mu_q/\rho_q)^{1/2}$ is the resonant

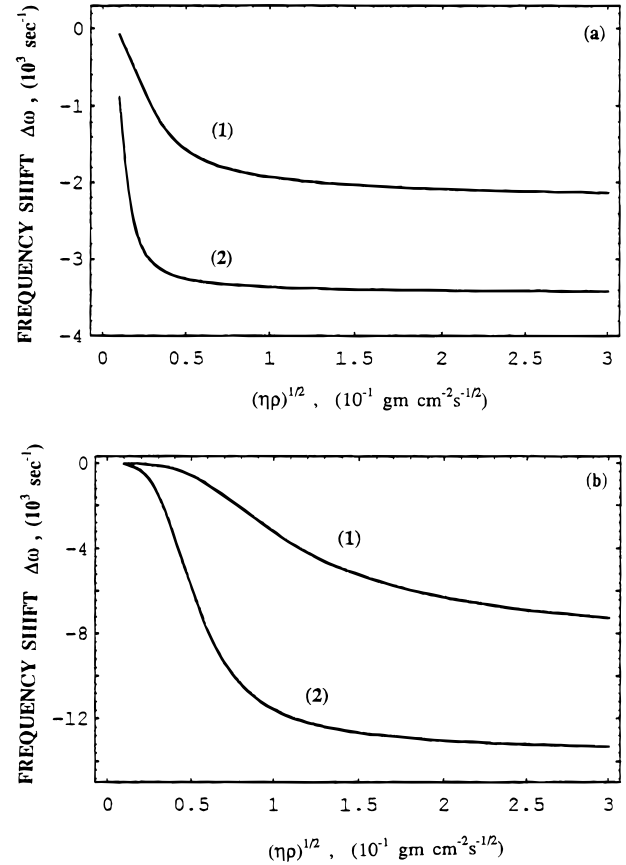


Figure 3. Layer-induced shift of the resonance frequency versus $(\eta\rho)^{1/2}$ (at fixed value $\rho = 1 \text{ g cm}^{-3}$) for two-layer thicknesses, 3a, $L = 0.5\delta_0$; 3b, $L = 2\delta_0$, where $\delta_0 = 250 \text{ nm}$ is the decay length of shear waves in water when the frequency is 5 MHz. The calculations were carried out for the following values of the parameters: $f = \omega_0/2\pi = 5 \text{ MHz}$ and (1) $\xi_H/L = 0.5$, (2) $\xi_H/L = 0.2$.

frequency of the uncoated smooth quartz crystal film operating in air. The first terms in the rhs of eqs 15 and 16 describe the QCM response for the smooth quartz crystal–bulk liquid interface.⁷ It should be mentioned that in this case the liquid-induced shift and width are equal. The additional terms present the shift and the width of the QCM resonance caused by the interaction of the liquid with the nonuniform interfacial layer.

Discussion

Let us focus on the limiting behaviors of eqs 15 and 16. When the permeability length scale is the shortest length of the problem, $\xi_H \ll \delta$ and $\xi_H \ll L$, eqs 15 and 16 reduce to

$$\Delta\omega = -\frac{\omega_0^2}{\pi(\mu_1 \rho_q)^{1/2}} \left(\left(\frac{\rho\eta}{2\omega_0} \right)^{1/2} + \rho(L - \xi_H) \right) \quad (17)$$

$$\Gamma = -\frac{\omega_0^2}{\pi(\mu_q \rho_q)^{1/2}} \left(\left(\frac{\rho\eta}{2\omega_0} \right)^{1/2} + \rho L \frac{\xi_H^2 \rho \omega_0}{\eta} \left(1 + \frac{1}{2L} \left(\frac{2\eta}{\rho \omega_0} \right)^{1/2} \right) \right) \quad (18)$$

We see that the layer-induced shift is proportional to the liquid density and does not depend on the viscosity. It has the form of the frequency shift due to a mass loading. The effect results from the inertial motion of the liquid trapped by the inhomogeneities in the interfacial layer. The effective thickness of the liquid film rigidly coupled

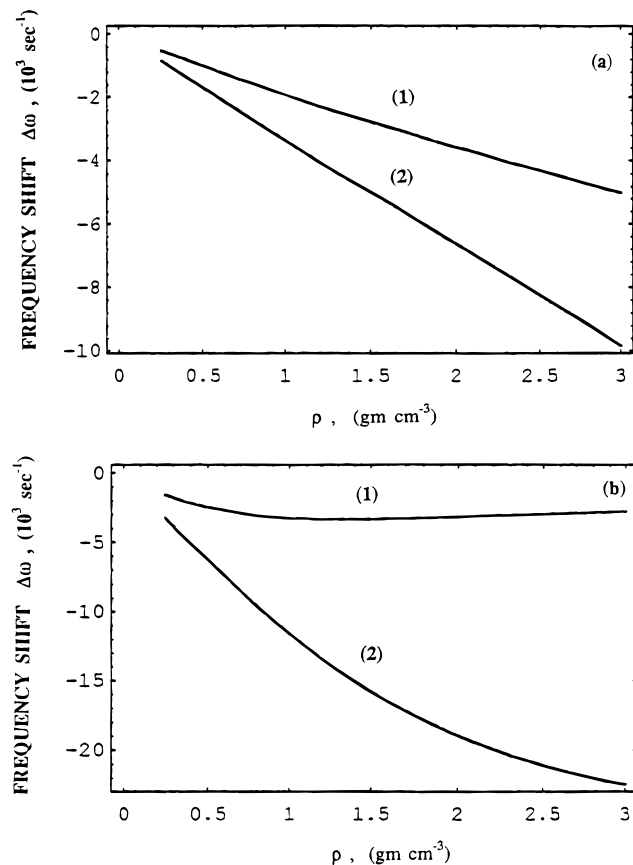


Figure 4. Layer-induced shift of the resonance frequency versus ρ (at fixed value $\eta = 1$ cP) for two-layer thicknesses, 4a, $L = 0.5\delta_0$; 4b, $L = 2\delta_0$, where $\delta_0 = 250$ nm is the decay length of shear waves in water when the frequency is 5 MHz. The calculations were carried out for the following values of the parameters: $f = \omega_0/2\pi = 5$ MHz and (1) $\xi_H/L = 0.5$, (2) $\xi_H/L = 0.2$.

to the oscillating surface is equal to $L - \xi_H$ and is less than the thickness of the inhomogeneous layer, L . This point must be taken into account in interpreting the QCM data. In the limiting case considered here, $\xi_H \ll \delta$ and $\xi_H \ll L$, the layer-induced correction to the width of the resonance is much less than the correction to the shift. The increase of the permeability ξ_H^2 leads to the enhancement of the velocity gradient in the layer (see Figure 2), which results in the decrease of the mass loading shift and in the increase of the width caused by the energy dissipation.

When the layer thickness is the shortest length of the problem, $L \ll \delta$, $L \ll \xi_H$, and $\xi_H \ll \delta$, eqs 15 and 16 can be rewritten in the form

$$\Delta\omega = -\frac{\omega_0^2}{\pi(\mu_q\rho_q)^{1/2}}\left\{\left(\frac{\rho\eta}{2\omega_0}\right)^{1/2} + \frac{1}{3}\rho L(L/\xi_H)^2\right\} \quad (19)$$

$$\Gamma = \frac{\omega_0^2}{\pi(\mu_q\rho_q)^{1/2}}\left\{\left(\frac{\rho\eta}{2\omega_0}\right)^{1/2} + \frac{1}{4}\rho L(L/\xi_H)^2\left(\frac{\rho\omega_0}{2\eta}\right)^{1/2} L\right\} \quad (20)$$

In this limit the layer-induced shift is also proportional to the liquid density and does not depend on viscosity. However, in contrast to the previous case, it cannot be related to the mass of trapped liquid. The correction to the width of the resonance depends on the viscosity, and it is substantially less than the layer-induced shift. We would like to stress that in both limiting cases discussed above the corrections to the shift and to the width of the resonance differ considerably. This difference has been ignored by the authors of ref 16 in interpreting of QCM measurements at rough surfaces.

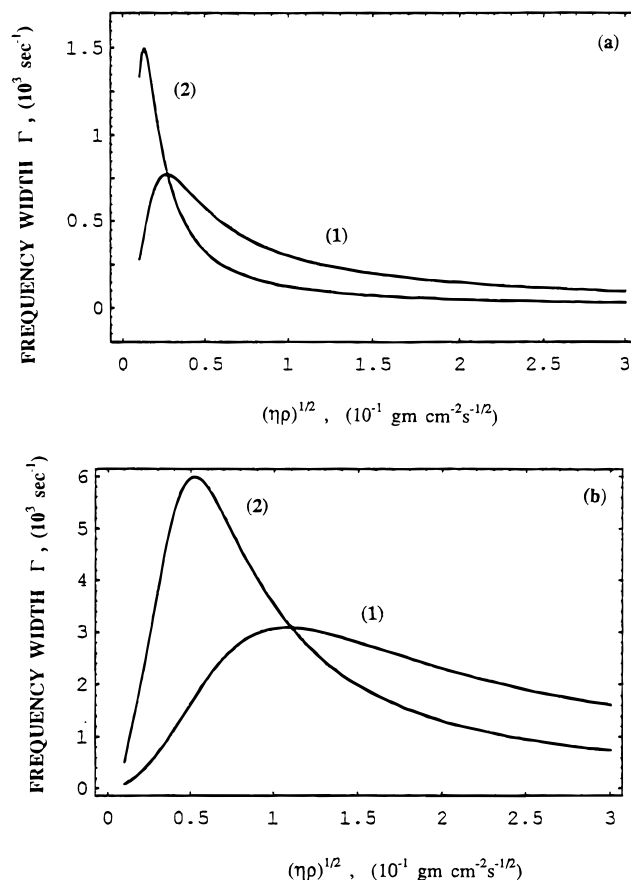


Figure 5. Layer-induced width of the resonance frequency versus $(\eta\rho)^{1/2}$ (at fixed value $\rho = 1$ g cm $^{-3}$) for two-layer thicknesses, 5a, $L = 0.5\delta_0$; b, $L = 2\delta_0$, where $\delta_0 = 250$ nm is the decay length of shear waves in water when the frequency is 5 MHz. The calculations were carried out for the following values of the parameters: $f = \omega_0/2\pi = 5$ MHz and (1) $\xi_H/L = 0.5$, (2) $\xi_H/L = 0.2$.

When the decay length δ is the longest length in the problem, $\delta \gg \xi_H$ and $\delta \gg L$, the following relationship between the shift and the broadening of the resonance due to the presence of the interfacial layer can be derived as

$$\frac{\Delta\omega - \Delta\omega_0}{(\Gamma - \Gamma_0)^{1/2}} \frac{1}{|\Delta\omega_0|^{1/2}} = \frac{\sqrt{2}(L/\xi_H - \tanh(L/\xi_H)) \cosh(L/\xi_H)}{\cosh(L/\xi_H) - 1} \quad (21)$$

where $\Delta\omega_0$ and Γ_0 are the shift and the width of the resonance at the smooth crystal–liquid interface

$$\Gamma_0 = -\Delta\omega_0 = \frac{\omega_0^2}{\pi(\mu_q\rho_q)^{1/2}}\left(\frac{\rho\eta}{2\omega_0}\right)^{1/2} \quad (22)$$

We see that the experimentally measurable ratio $(\Delta\omega - \Delta\omega_0)/(\Gamma - \Gamma_0)^{1/2}$ depends on the single intrinsic characteristic of the interfacial layer, ξ_H/L . Equation 21 can be used to estimate the permeability ξ_H^2 from the experimental data. For $L/\xi_H \ll 1$ and $L/\xi_H \gg 1$ the rhs of eq 21 reduces to the following simple expressions $(2\sqrt{2}/3)L/\xi_H$ and $\sqrt{2}L/\xi_H$, correspondingly.

The usual form of the description of the experimental data in liquids is the representation of the real and imaginary components of QCM response as functions of

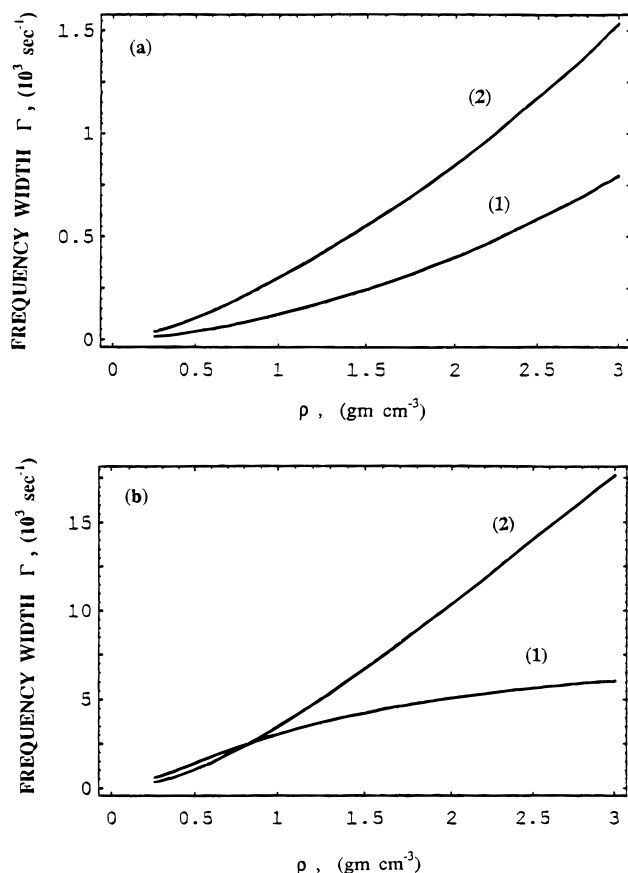


Figure 6. Layer-induced width of the resonance frequency versus ρ (at fixed value $\eta = 1$ cP) for two-layer thicknesses, 6a, $L = 0.5\delta_0$; 6b, $L = 2\delta_0$, where $\delta_0 = 250$ nm is the decay length of shear waves in water when the frequency is 5 MHz. The calculations were carried for the following values of the parameters: $f = \omega_0/2\pi = 5$ MHz and (1) $\xi_H/L = 0.5$, (2) $\xi_H/L = 0.2$.

the liquid density ρ and of the parameter $(\rho\eta)^{1/2}$. Figures 3–6 show the dependencies of the layer-induced shift and the width of the resonance frequency on ρ and $(\rho\eta)^{1/2}$, which have been calculated according to eqs 15 and 16. The common features of all curves are the increase of the QCM-response with the increase of the film thickness and with the decrease of the ratio ξ_H/L . The frequency shift changes rapidly with $(\rho\eta)^{1/2}$ in the region of $(\rho\eta)^{1/2} < t_*(L/\delta, \xi_H/L)$, where the limiting value t_* is of the order of unity, and slowly increases with the increase of the parameters L/δ and ξ_H/L . For higher values of $(\rho\eta)^{1/2}$ the function $\Delta\omega((\rho\eta)^{1/2})$ tends to a constant (see Figure 3). This behavior reflects the fact that in the high viscosity limit, when $L/\delta \ll 1$, the gradient of the velocity in the interfacial layer is small and the layer influences only slightly the velocity field in the bulk liquid. As a result, the viscosity-dependent contribution to the frequency shift, which is proportional to the velocity gradient, would remain the same as for the smooth solid–liquid interface. This point also explains the decrease of the layer-induced width of the resonance with increasing $(\rho\eta)^{1/2}$ for $(\rho\eta)^{1/2} > t_*(L/\delta, \xi_H/L)$ (see Figure 5). We remark that the plots $\Delta\omega$ versus $(\rho\eta)^{1/2}$ presented on Figure 3 closely resemble the plots that have been obtained for slightly rough surfaces within the perturbation approach.²² The predicted dependencies of $\Delta\omega$ on $(\rho\eta)^{1/2}$ agree qualitatively with experimental data¹⁵ found for rough solid surfaces in contact with methanol–water mixtures and alcohols.

Figure 4 shows that the frequency shift is linear in the liquid density for small thicknesses of the interfacial layer, $L/\delta \ll 1$, and the deviations from the linear proportionality

arise as the thickness increases. The deviations are caused by the increase of the contribution of the energy dissipation processes to the QCM response with the increase of the thicknesses.

Our calculations predict the interesting feature of the layer-induced width of the resonance as a function of $(\rho\eta)^{1/2}$ (see Figure 5). For $L \geq \delta$ the curves for Γ versus $(\rho\eta)^{1/2}$ have the maxima located at $(\rho\eta)^{1/2} \approx t_*(L/\delta, \xi_H/L)$. The appearance of the maxima results from the fact that the energy dissipation induced by the interfacial layer diminishes for both high and low viscosities. This effect has been already discussed above. The dependencies of the resonance width on the liquid density shown on Figure 6 reflect the influence of both the mass loading and the energy dissipation contributions. For the thin layers the curves Γ versus ρ have the quadratic form, as predicted by eq 20.

Our model demonstrates that in the case of polymer films being in contact with a liquid the QCM response strongly depends on the thickness of the film and on the correlation length. These parameters are changed drastically under phase transitions. The QCM response of the amphoteric polymer film undergoing phase transitions between the isoelectric and the cationic and anionic forms has been studied in ref 35. Large resonance frequency shifts, which are not consistent with the mass changes, have been observed for polymer films in the vicinity of the phase transition point.³⁵ The phase measurement interferometric microscopy demonstrated that phase transitions were accompanied by dramatic changes in the film thickness. Our model explains the observed effect by the variation of the thickness or/and correlation length of the polymers film under phase transition. In order to estimate the changes of the film thickness and of the correlation length both the real and the imaginary part of QCM response should be measured.

Conclusions

A new approach for the description of the effect of surface roughness on the QCM response in contact with a liquid has been proposed. The approach is based on Brinkman's equation for the velocity field in the nonuniform interfacial region. Within our model the roughness-induced shift and width of the resonant frequency are determined by two parameters: δ/L and ξ_H/L . They are the ratios of the decay length of the shear wave in the liquid and the permeability length scale in the interfacial layer to the thickness of this layer. The frequency changes due to both the inertial motion of a liquid rigidly coupled to the surface and due to the additional viscous energy dissipation induced by roughness have been found. The results obtained are as follows:

(1) In the case of thin rough layers, $L < \delta$, the resonant frequency decreases rapidly with the increase of $(\rho\eta)^{1/2}$. When L approaches δ , the resonant frequency loses the dependence on $(\rho\eta)^{1/2}$ and tends to a constant. This behavior agrees with the results derived within the perturbation approach.²² The linear dependence of the frequency shift on the liquid density has been found for $L < \delta$. The slope of the lines $\Delta\omega$ versus ρ increases with the decrease of the parameter ξ_H^2/L . For, $L \geq \delta$, the dependence of the shift on the liquid density becomes more complicated.

(35) Wang, J.; Ward, M. D.; Ebersole, R. C.; Foss, R. P. *Anal. Chem.* **1993**, *65*, 2553.

(2) Our calculations predict that the roughness-induced width of the resonance, Γ , has a maximum as a function of $(\rho\eta)^{1/2}$. The position of the maximum moves to lower values of $(\rho\eta)^{1/2}$ with the decrease of the thickness of the interfacial layer. The roughness-induced width increases with the increase of the liquid density. For thin interfacial layers, $L < \delta$, curves Γ versus ρ have a quadratic form.

(3) Our calculations demonstrate that while for smooth surfaces liquid-induced shift and width of the resonance are equal they differ essentially for rough surfaces. This effect, ignored by the authors of ref 16, has been observed in ref 20. Our results show that empirical representation of the QCM response in a liquid as a linear combination of a $(\rho\eta)^{1/2}$ and a ρ terms²⁰ can be applied for the description of the shift of the resonant frequency in the case of thin rough layers, $L < \delta$.

Appendix

Using eqs 5–7 and Brinkman's equation (2) one can present the energy balance in the form

$$\begin{aligned} \frac{d}{dt}(E_{\text{kin}}^{(q)} + U^{(q)} + E_{\text{kin}}^{(s)} + E_{\text{kin}}^{(b)}) = & \mu_q V_0 \times \\ & \exp(i\omega t) \frac{\partial}{\partial z} u_x(z, t) \Big|_{z=d} + \eta \xi_H^{-2} \int_d^L dz v_x(z, t) (V_0 \exp(i\omega t) - \\ & v_x(z, t) + \eta \left[v_x(z, t) \frac{\partial}{\partial z} v_x(z, t) \right] \Big|_{z=L-0} - \\ & \left[v_x(z, t) \frac{\partial}{\partial z} v_x(z, t) \right] \Big|_{z=d} - \eta \int_d^L dz \left(\frac{\partial}{\partial z} v_x(z, t) \right)^2 - \\ & \eta \left(v_x(z, t) \frac{\partial}{\partial z} v_x(z, t) \right) \Big|_{z=L+0} - \eta \int_L^\infty dz \left(\frac{\partial}{\partial z} v_x(z, t) \right)^2 \quad (\text{A.1}) \end{aligned}$$

The boundary conditions (b) and (c) for the velocity field result in the compensation of the energy fluxes through

the interface $z = L$. Hence, eq A.1 can be reduced to

$$\begin{aligned} \frac{d}{dt}(E_{\text{kin}}^{(q)} + U^{(q)} + E_{\text{kin}}^{(s)} + E_{\text{kin}}^{(b)}) = & \\ & -\eta \int_d^L dz \left(\frac{\partial}{\partial z} v_x(z, t) \right)^2 - \eta \int_L^\infty dz \left(\frac{\partial}{\partial z} v_x(z, t) \right)^2 - \\ & \eta \xi_H^{-2} \int_d^L dx (V_0 \exp(i\omega t) - v_x(z, t))^2 + \\ & \mu_q V_0 \exp(i\omega t) \frac{\partial}{\partial z} u_x(z, t) \Big|_{z=d} + \eta \xi_H^{-2} V_0 \exp(i\omega t) \int_d^L dz \times \\ & (V_0 \exp(i\omega t) - v_x(z, t) - \eta \left[v_x(z, t) \frac{\partial}{\partial z} v_x(z, t) \right] \Big|_{z=d}) \quad (\text{A.2}) \end{aligned}$$

The first and the second terms in rhs of eq A.2 describe the viscous dissipation in the interfacial layer and in the bulk, respectively. The third, negatively defined term in eq A.2 can be interpreted as an additional dissipation due to interactions between the liquid and solid phases in the layer. The remaining terms in the rhs of eq A.2 can be rewritten as

$$\begin{aligned} V_0 \exp(i\omega t) \left[\mu_q \frac{\partial}{\partial z} u_x(z, t) \Big|_{z=d} - \eta \frac{\partial}{\partial z} v_x(z, t) \Big|_{z=d} + \right. \\ \left. \eta \xi_H^{-2} \int_d^L dz (V_0 \exp(i\omega t) - v_x(z, t)) \right] \quad (\text{A.3}) \end{aligned}$$

The first and the second terms in the brackets are the shear stresses at the surface $z = d$ that arise from oscillations of the quartz crystal and the liquid. The last term describes the integral stress that results from the liquid–solid interactions in the layer and is transmitted through the rigid phase to the quartz crystal surface, $z = d$. Since the net stress applied to the interface $z = d$ should be zero, eq A.2 reduces to eq 4 in the text.

LA950763D